

Article

Bioassay-Guided Isolation of Two Eudesmane Sesquiterpenes from *Lindera strychnifolia* Using Centrifugal Partition Chromatography

Ji Hoon Kim ^{1,†}, Je-Seung Jeon ^{1,†}, Jung Hoon Kim ¹, Eun Ju Jung ¹, Yun Jung Lee ¹, En Mei Gao ¹, Ahmed Shah Syed ², Rak Ho Son ^{1,3} and Chul Young Kim ^{1,*} 

- ¹ College of Pharmacy, Institute of Pharmaceutical Science and Technology, Hanyang University, Ansan 15588, Korea; gg890718@gmail.com (J.H.K.); jsjeoncy@gmial.com (J.-S.J.); evveje@naver.com (J.H.K.); jejs2@naver.com (E.J.J.); sopihya@naver.com (Y.J.L.); rhdmsal@hanyang.ac.kr (E.M.G.); sonnaco@huons.com (R.H.S.)
- ² Department of Pharmacognosy, Faculty of Pharmacy, University of Sindh, Jamshoro 76080, Pakistan; shahahmed454@gmail.com
- ³ R&D Center, Huons Co., Ltd., Ansan 15588, Korea
- * Correspondence: chulykim@hanyang.ac.kr; Tel.: +82-31-400-5809
- † These authors contributed equally to this work.

Abstract: In this study, a centrifugal partition chromatography (CPC) separation was applied to identify antioxidant-responsive element (ARE) induction molecules from the crude extract of *Lindera strychnifolia* roots. CPC was operated with a two-phase solvent system composed of *n*-hexane-methanol-water (10:8.5:1.5, *v/v/v*) in dual mode (descending to ascending), which provided a high recovery rate (>95.5%) with high resolution. Then, ARE induction activity of obtained CPC fractions was examined in ARE-transfected HepG2 cells according to the weight ratios of the obtained fractions. The fraction exhibiting ARE-inducing activity was further purified by preparative HPLC that led to isolation of two eudesmane type sesquiterpenes as active compounds. The chemical structures were elucidated as linderolide U (**1**) and a new sesquiterpene named as linderolide V (**2**) by spectroscopic data. Further bioactivity test demonstrated that compounds **1** and **2** enhanced ARE activity by 22.4-fold and 7.6-fold, respectively, at 100 μ M concentration while 5 μ M of sulforaphane induced ARE activity 24.8-fold compared to the control.

Keywords: *Lindera strychnifolia*; centrifugal partition chromatography; linderolide V; eudesmane sesquiterpenes



Citation: Kim, J.H.; Jeon, J.-S.; Kim, J.H.; Jung, E.J.; Lee, Y.J.; Gao, E.M.; Syed, A.S.; Son, R.H.; Kim, C.Y. Bioassay-Guided Isolation of Two Eudesmane Sesquiterpenes from *Lindera strychnifolia* Using Centrifugal Partition Chromatography. *Molecules* **2021**, *26*, 5269. <https://doi.org/10.3390/molecules26175269>

Academic Editor: Nicola Marchetti

Received: 4 August 2021

Accepted: 25 August 2021

Published: 30 August 2021

Publisher's Note: MDPI stays neutral with regard to jurisdictional claims in published maps and institutional affiliations.



Copyright: © 2021 by the authors. Licensee MDPI, Basel, Switzerland. This article is an open access article distributed under the terms and conditions of the Creative Commons Attribution (CC BY) license (<https://creativecommons.org/licenses/by/4.0/>).

1. Introduction

Natural products are a pool of molecules that attract pharmaceutical interest. To search interesting bioactive compounds from natural extracts, performing a bioassay-guided fractionation that gears toward silica-based chromatographic steps is common. During the isolation workflow, however, innate physicochemical properties of its solid-like packing materials often bring about loss of activity or failure in isolation concomitant with insufficient concentration of target compounds for bioactivity test [1,2]. Thus, a fractionation system that enhances separation efficiency and total sample recovery while lowering the risk in sample denaturation is needed. For this purpose, counter-current separations are an efficient chromatographic tool to combine with bioactivity tests. Centrifugal partition chromatography (CPC) is a type of support-free liquid-liquid chromatography technique that uses an immiscible two-phase solvent system to compose stationary and mobile phase. CPC offers many advantages such as a higher sample loading capacity, the absence of sample loss due to irreversible sample absorption to the solid column, a flexible operation mode, and the choice of a wide range of solvent systems [3–12], so it can achieve the fractionations with sufficient amount to further in vitro bioactivity tests [11,12].

Lindera strychnifolia Fernandez-Villar (Lauraceae) is an evergreen shrub that is widely distributed in Asia. As *Lindera* root is known to stimulate Qi circulation, eliminate cold and pain, it has been used in the treatment of stomach and renal diseases, neuralgia, and rheumatism in traditional Oriental medicine [13]. Recent studies also reported antioxidant, anti-diabetic, and anti-inflammatory effects of *Lindera* root. Sesquiterpenes are major constituents of this plant, and alkaloids and tannins are also isolated [14–17]. The crude extract of the root of *L. strychnifolia* enhanced the antioxidant response element (ARE) activity in an ongoing screening for natural products in HepG2-ARE luciferase assay.

In this study, the dual-mode CPC was applied to obtain high-resolution fractions of *L. strychnifolia* extract and obtained fractions were tested in ARE-inducing activity in accordance with the weight ratio of fractions. The active fraction was further purified by preparative HPLC to isolate two eudesmane sesquiterpenes exhibiting ARE-inducing activities.

2. Results

2.1. Isolation of Active Compounds Using Dual-Mode CPC and HPLC

When the preliminary experiment was carried out using linear-gradient CPC to identify active peaks from nonpolar to polar fractions, nonpolar fraction-exerted ARE induction activity and comparison of an active fraction and *n*-hexane extract was revealed similar HPLC chromatograms (Supplementary Materials Figures S1–S4). Therefore, *n*-hexane extract was chosen for further purification. HPLC analysis in Figure 1 presented several major peaks a–e, which were used for the calculation of partition coefficient (*K* value).

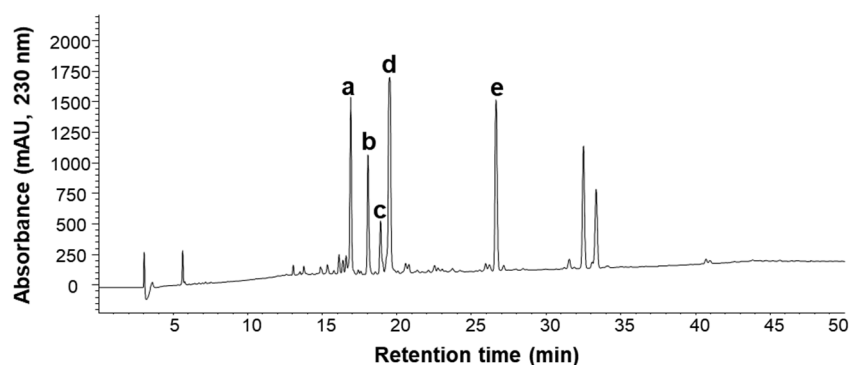


Figure 1. HPLC chromatogram of *n*-hexane extract of *L. strychnifolia*.

After calculation of *K* values of major peaks a–e, a two-phase solvent system with *n*-hexane-methanol-water (10:8.5:1.5, *v/v/v*) was selected (Table 1).

Table 1. The *K* values of major peaks a–e in *n*-hexane extract in different solvent systems.

Solvent System (<i>v/v/v</i>) <i>n</i> -Hexane:Methanol:Water	Partition Coefficient (<i>K</i> ¹)				
	Peak a	Peak b	Peak c	Peak d	Peak e
10:9.5:0.5	5.47	4.22	3.90	2.86	0.67
10:9:1	5.02	3.51	3.67	2.15	0.45
10:8.5:1.5	4.28	2.65	2.78	1.84	0.29
10:8:2	2.29	1.54	1.46	1.06	0.17

¹ *K* value = peak area of upper phase/peak area of lower phase.

Dual-mode CPC was applied to recover all introduced samples with high-resolution. The upper organic phase was firstly eluted as the mobile phase. After 230 min operation in ascending mode, elution was changed to descending mode to recover remaining samples in the rotor and maintained to 345 min.

As shown in Figure 2, ten fractions (H1–H10) were obtained: H1 (30–45 min, 940.8 mg), H2 (45–100 min, 964.1 mg), H3 (100–170 min, 89.1 mg), H4 (170–230 min, 114.0 mg), H5

(230–235 min, 550.4 mg), **H6** (235–250 min, 417.5 mg), **H7** (250–255 min, 45.2 mg), **H8** (255–270 min, 339.8 mg), **H9** (270–305 min, 1226.5 mg), and **H10** (305–345 min, 88.9 mg). The total sum of each fraction was 4776.3 mg out of 5.0 g of crude sample, exhibiting 95.5% recovery rate. Next, each fraction was evaluated for the ARE-inducing activity at a concentration of 30 $\mu\text{g}/\text{mL}$, and ten fractions were evaluated at the concentration applied at each assigned weight ratio (Table 2).

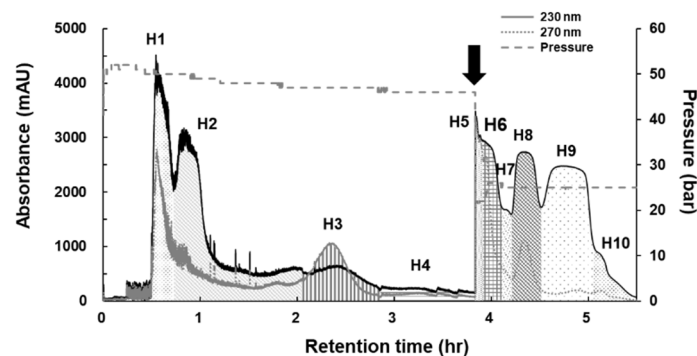


Figure 2. Dual mode CPC chromatogram of *n*-hexane extract of *L. strychnifolia*. The details are described in Section 3.6 CPC procedure.

Table 2. Fraction weights and calculated concentrations.

Fractions	H1	H2	H3	H4	H5	H6	H7	H8	H9	H10	Sum
Weight (mg)	940.8	964.1	89.1	114.0	550.4	417.5	45.2	339.8	1226.5	88.9	4776.3
Weight ratio (%)	19.7	20.2	1.9	2.4	11.5	8.7	0.9	7.1	25.7	1.9	100
Treatment ($\mu\text{g}/\text{mL}$)	5.91	6.06	0.56	0.72	3.46	2.62	0.28	2.13	7.70	1.86	30

As shown in Figure 3, the results showed that fraction **H9** exerted the highest activity. HPLC analysis revealed that **H9** fraction contained two major peaks, **1** and **2**. Further purification by prep-HPLC led to the isolation of compounds **1** and **2**. The following section will describe structural elucidations.

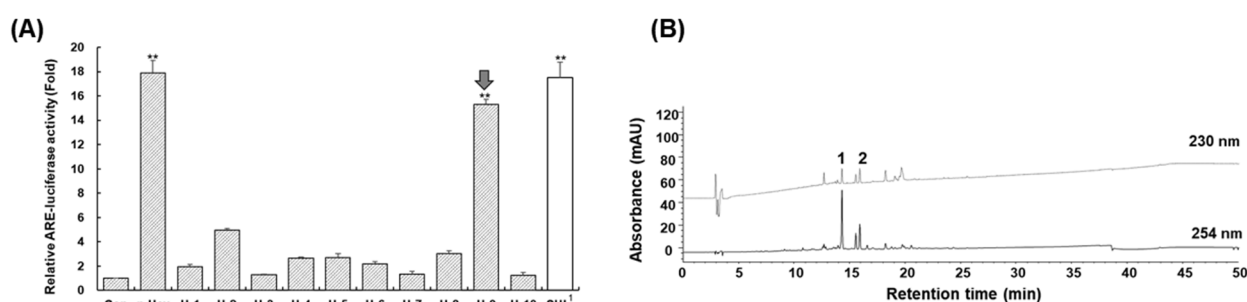


Figure 3. The relative antioxidant response element (ARE)-luciferase activities (A) of the CPC-fractions **H1H10** and HPLC chromatogram (B) of active fraction **H9**. The ARE induction activities were evaluated in ARE-HepG2 cells at concentrations applied at each assigned weight ratio (based on 30 $\mu\text{g}/\text{mL}$ of crude extract). Data are presented as the mean \pm S.E. ($n = 3$). ** $p < 0.01$ (compared with the vehicle-treated control). ¹ Sulforaphane was treated 5 μM as positive control.

2.2. Structural Elucidation of Compounds **1** and **2**

Chemical structures of purified compounds were determined by spectroscopic methods, including NMR (^1H , ^{13}C NMR, COSY, HSQC, HMMC, NOESY and Mosher's method) and HR-ESI-MS spectral data (Table 3).

Compound **1** was isolated as a brownish powder. Its molecular formula was determined as $\text{C}_{16}\text{H}_{20}\text{O}_4$ by the HR-ESI-MS ion at m/z 299.1242 $[\text{M} + \text{Na}]^+$. Analysis of the ^{13}C and HSQC spectra of **1** revealed 16 carbon signals that attributed to two methyls (at δ_{C} 17.9

and 20.2), one methoxy (at δ_C 52.8), two methylenes (at δ_C 17.6, 54.4), one *exo*-methylene (at δ_C 108.6), three methines (at δ_C 29.1, 24.4 and 67.2), one oxygenated methine (at δ_C 65.9), and six quaternary carbons. In the ^1H NMR spectrum, two methyl signals at δ_H 0.74 and 2.10 (each 3H), one methoxyl at δ_H 3.72 (3H, s), one hydroxymethine at δ_H 4.42 (1H, dd, $J = 11.0, 0.9$), and three methines at δ_H 1.45 (1H, ddd, $J = 8.0, 7.1, 3.6$), 2.04 (1H, m) and 2.79 (1H, ddd, $J = 11.0, 3.2, 2.2$) were observed. Besides, the presence of *exo*-methylene was easily deduced from resonances at δ_H 5.10 (1H, dt, $J = 2.6, 1.4$ Hz) and 5.24 (1H, d, $J = 1.4$ Hz) connected to δ_C 108.6 in the HSQC spectrum. In the ^1H - ^1H COSY spectrum, the connections of -CH(H-1)-CH₂(H-2)-CH(H-3)- and CH(H-5)-CH(H-6) were observed; especially, long-range couplings of H-15 and H-5, H-13 and H-6 were detected. In the HSQC spectrum, one oxymethine carbon was observed at δ_C 65.9, connected to δ_H 4.42 (1H, dd, $J = 11.0, 0.9$). Besides, three methines were also revealed at δ_C 29.1, 24.4 and 67.2, corresponding to δ_H 1.45 (1H, dd, $J = 11.0, 1.2$), 2.04 and 2.79, respectively. In the HMBC spectrum, correlations were observed between from H-15 to C-3/C-3/C-4, from H-14 to C-1/C-5/C-9/C-10, from H-13 to C-7/C-11/C-12, from H-2 to C-1/C-3/C-10 and from H-9 to C-8/C-10. The HMBC spectrum showed a correlation between δ_H 2.10 (H-13), 3.72 (OCH₃) and a carbonyl resonance at δ_C 173.5 (C-12), and between δ_H 2.58 (H-9), 4.42 (H-6) and a carbonyl signal at δ_C 202.36 (C-8), showing similarity to those of a side chain in linderolides L and M [15]. The relative stereochemistry of **1** was determined by NOESY, which showed correlations between Me-14 and H-6, which suggested that these protons exist on the same side. The NOESY correlation between H-6 and CH₃-13 suggested a *Z*-configuration of the 7,11 double bond. The absolute configuration at the 6-position of **1** was determined to be *S* by a modified Mosher's method (Supplementary Materials Figure S11) [18]. Based on the obtained data, compound **1** was determined as linderolide U (Figure 4). Recently, linderolide U was identified in this plant [19].

Table 3. ^1H (400 MHz) and ^{13}C NMR (100 MHz) data for compounds **1** and **2** in CD₃OD (δ in ppm, J values in parentheses).

No.	Linderolide U (1)		Linderolide V (2)	
	^1H (J in Hz)	^{13}C	^1H (J in Hz)	^{13}C
1	1.45 (ddd, $J = 8.0, 7.1, 3.6$)	29.1 CH	1.52 (dt, $J = 7.5, 3.9$)	28.4 CH
2	0.90 (ddd, $J = 8.9, 8.0, 5.2$), 0.81 (dt, $J = 5.2, 3.6$)	17.6 CH ₂	0.88 (ddd, $J = 10.7, 7.9, 4.2$)	18.5 CH ₂
3	2.04 (m)	24.4 CH	1.98 (t, $J = 9.4$)	23.7 CH
4		152.0 C		151.3 C
5	2.79 (ddd, $J = 11.0, 3.2, 2.2$)	67.2 CH	2.69 (dt, $J = 9.6, 2.6$)	67.4 CH
6	4.42 (dd, $J = 11.0, 0.9$)	65.9 CH	4.10 (d, $J = 9.6$)	64.1 CH
7		139.9 C		120.9 C
8		202.3 C		151.2 C
9	2.58 (dd, $J = 4.3, 0.9$)	54.4 CH ₂	2.59 (dt, $J = 16.3, 3.5$), 2.36 (d, $J = 16.3$)	38.1 CH ₂
10		37.7 C		40.6 C
11		146.0 C	3.37 (m)	39.8 CH
12		173.5 C		181.7 C
13	2.10 (d, $J = 0.9$)	17.9 CH ₃	1.33 (d, $J = 7.6$)	14.3 CH ₃
14	0.74 (s)	20.2 CH ₃	0.71 (s)	17.3 CH ₃
15	5.24 (d, $J = 1.4$), 5.10 (dt, $J = 2.7, 1.4$)	108.6 CH ₂	5.20 (brs), 5.06 (d, $J = 1.2$)	108.6 CH ₂
OCH ₃	3.72 (s, 3H)	52.8 CH ₃		

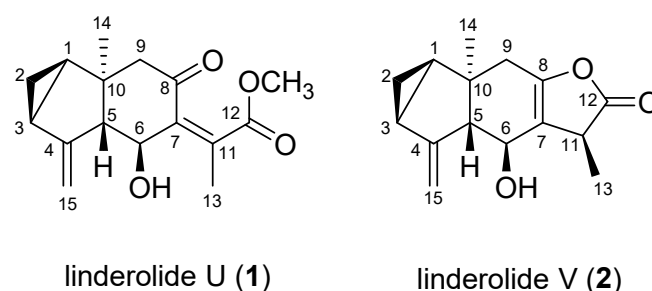


Figure 4. Chemical structures of isolated compounds **1** and **2**.

Linderolide V (**2**) was isolated as a brown powder, and its molecular formula was determined to be $C_{15}H_{18}O_3$ based on HR-QTOF/MS at m/z 269.1231 $[M + Na]^+$. The ^{13}C and HSQC spectra revealed 15 carbon signals that attributed to two methyls (at δ_C 17.3 and 14.3), three methylenes (at δ_C 18.56, 38.1, 108.6), three methines (at δ_C 28.4, 23.7 and 67.4), one oxymethine (at δ_C 64.1), and five quaternary carbons. In the 1H NMR spectrum, two methyl signals at δ_H 0.71 (s) and 1.33 (d), one hydroxymethine at δ_H 4.10 (1H, d, $J = 9.6$), three methines at δ_H 1.52 (1H, dt, $J = 7.5, 3.9$), 1.98 (1H, t, 9.4) and 3.37 (1H, m), and characteristic *exo*-methylene resonances at δ_H 5.06 and 5.20 were observed. The correlations of $-CH(H-1)-CH_2(H-2)-CH(H-3)-$ and $-CH(H-5)-CH(H-6)$ were observed in the $^1H-^1H$ COSY spectrum.

In the HSQC spectrum, one oxymethine carbon was observed at δ_C 64.1, connected to δ_H 4.10 (1H, d, $J = 9.62$). Besides, three methines were also revealed at δ_C 28.4, 23.7 and 67.4, corresponding to δ_H 1.52 (1H, dt, $J = 7.5, 3.9$), 1.98 and 2.69, respectively. In the HMBC spectrum, correlations were observed from H-15 to C-3/C-5/C-4, from H-14 to C-1/C-5/C-10, from H-13 to C-7/C-11/C-12, from H-2 to C-1/C-3/C-4/C-10 and from H-9 to C-2/C-5/C-7/C-8/C-10, from H-6 to C-7/C-8. The chemical structure of **2** was similar to the previously reported compound, shizukanolide [20], but the double bond position C-7/C11 was changed to C7/C8 (Figure 4). Based on the obtained data, compound **2** was determined as shown in Figure 4 and was named linderolide V.

The relative stereochemistry of **2** was determined by NOESY, which showed correlations between CH_3 -14 and H-6 which suggested that these protons exist on the same side. CH_3 -13 and H-5 also showed a correlation that means these protons are on the same side. However, CH_3 -13 and CH_3 -14 did not show any correlations that are located on the opposite side (Figure 5). The coupling constant between H-5/H-6 was 9.6 Hz which supported that H-5 and H-6 were located on the other side. In addition, the $\Delta\delta$ values between the (*S*) and (*R*)-MTPA esters indicated the 6*S* configuration for **2** (Supplementary Materials Figure S19) [18].

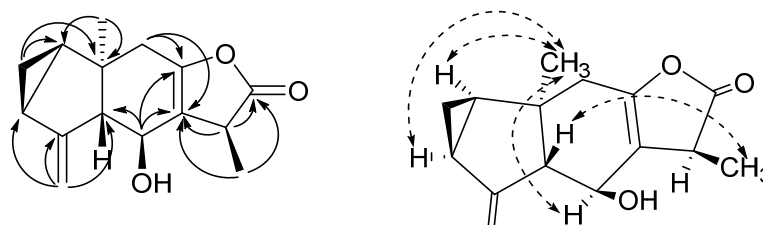


Figure 5. Key HMBC ($H \rightarrow C$) and NOESY ($H \leftrightarrow H$) correlations of compound **2**.

2.3. Induction of Antioxidant Response Element by Compounds **1** and **2**

The ARE-inducing ability of the isolated compounds **1** and **2** from an active fraction (**H9**) were assessed by luciferase assay in HepG2 cells at a serial concentration of 3, 10, 30, and 100 μ M. Linderolide U (**1**) and linderolide V (**2**) enhanced ARE activity in a dose-dependent manner (Figure 6). At 100 μ M concentration, Compounds **1** and **2** enhanced ARE activity 22.4-fold and 7.6-fold, respectively, while 5 μ M of sulforaphane induced ARE activity 24.8-fold. These results indicated that compounds **1** and **2** were active principles for ARE induction of *L. strychnifolia*.

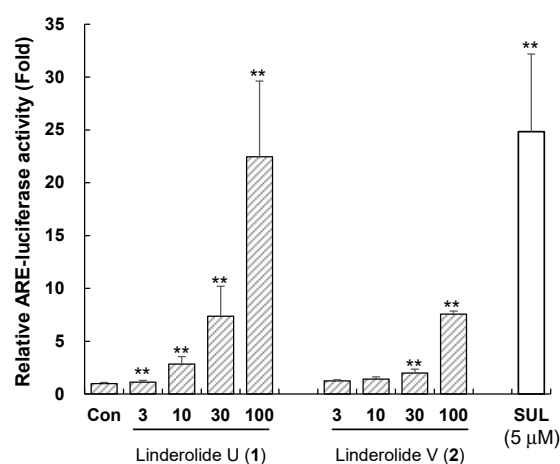


Figure 6. The relative antioxidant response element (ARE)-luciferase activities of isolated compounds 1 and 2. The ARE induction activities were evaluated in ARE-HepG2 cells at concentrations applied at each assigned weight ratio (based on 30 $\mu\text{g}/\text{mL}$ crude extract. Data are presented as the mean \pm S.E. ($n = 3$). ** $p < 0.01$ (compared with the vehicle-treated control). SUL: Sulforaphane was treated as a positive control.

3. Materials and Methods

3.1. Apparatus

An Armen fully integrated SCPC-100 + 1000 CPC spot instrument (Armen Instruments, St-Ave, France) was used in this study. This instrument is a fully automated system consisting of a CPC column compartment (1000 mL rotor made of 21 stacked disks with a total of 1512 twin cells), a pump, an injector, a UV/vis detector, a fraction collector, a digital screen flat PC and Armen Glider CPC software. The HPLC analysis was performed by an Agilent 1260 HPLC system (Agilent Technologies, Palo Alto, CA, USA): G1312C binary pump, a G1329B autosampler, a G1315D DAD detector, a G1316A column oven, and ChemStation software.

3.2. Chemicals and Reagents

All solvents used for the CPC were of analytical grade and purchased from Daejung Chemical (Korea). The HPLC-grade solvents were obtained from Fisher Scientific (Pittsburgh, PA, USA). The *L. strychnifolia* roots, well dried and sliced around 2 mm, were purchased from the Kyungdong Oriental herbal market, Seoul, Republic of Korea, in January 2018. A voucher specimen (HYUP-LS-001) was deposited in the Herbarium of the College of Pharmacy, Hanyang University (Supplementary Materials Figure S1).

3.3. Preparation of Crude Samples

Dried and coarsely ground sample (600 g of *L. strychnifolia* roots) was extracted with methanol by reflux for 2 h. The extraction was repeated three times and combined. The filtrate was evaporated under reduced pressure using a rotary evaporator to obtain 12.5 g of crude extract. Ten grams of crude extract was dissolved in water and extracted with 500 mL *n*-hexane three times. After dryness, 5.4 g of *n*-hexane extract was obtained.

3.4. HPLC Analysis

The crude extract and its CPC peak fraction were profiled by HPLC equipped with a Capcellpak UG120 C18 column (4.6 \times 250 mm, 5 μm , Shiseido, Tokyo, Japan). The mobile phase was composed of acetonitrile containing 0.1% formic acid (A) and water containing 0.1% formic acid (B). The gradient elution conditions were as follows: 0–10 min, 10–50% A; 10–45 min, 50–95% A; and 50 min, 95% A. The column temperature was 40 $^{\circ}\text{C}$, the mobile phase flow rate was 1 mL/min, the detection wavelength was 230 and 254 nm and the injection volume was 10 μL .

3.5. Selection of Solvent System

Because *n*-hexane extract was nonpolar, a series of solvent systems of *n*-hexane-methanol-water were tested. Briefly, approximately 2 mg of the sample was added to each test tube, 2 mL of each phase of a pre-equilibrated two-phase solvent system was added, and they were thoroughly mixed. After equilibration, 100 μ L of the upper and lower phases were added to 900 μ L methanol, and 10 μ L were analyzed by HPLC at 230 nm. The *K* values of major peaks (a–e) were described as the peak area of each compound in the upper stationary phase divided by that of the lower mobile phase.

3.6. CPC Operation for Active *n*-Hexane Extract

n-Hexane extract was purified by CPC operation with a two-phase solvent system composed of *n*-hexane-methanol-water (10:8.5:1.5, *v/v/v*) according to the *K* values of major peaks a–e (Table 1). The lower aqueous phase was used as mobile phase and the upper organic phase as stationary phase with ascending mode. The 1000 mL volume of the CPC rotor was filled with a lower layer at 50 mL/min in ascending mode at a speed of 500 rpm. Then, the rotation speed of the rotor was accelerated to 1000 rpm, and the upper layer as the mobile phase was carried into the rotor in descending mode at a flow rate of 10 mL/min. After the equilibration between the upper phase and lower phase was established, the sample solution (5.0 g) was loaded into CPC system, and the effluents were continuously monitored by a UV detector at 230 and 254 nm. After 230 min operation in ascending mode, elution was changed to descending mode to recover remaining samples in the rotor and maintain to 330 min.

3.7. Isolation and Structural Elucidation of Active Compounds 1 and 2

After CPC operation and evaluation of ARE-inducing activity, subfraction H9 was further purified by preparative HPLC. HPLC was carried out using a Gilson 321 pump, a Waters 2487 detector, an RS Tech HECTOR C18 column (5 μ m, 250 \times 21.2 mm, RS Tech Corp, Cheongju, South Korea). Isocratic elution mode (40% acetonitrile) at a flow rate of 10 mL/min was used and monitored at 230 and 254 nm. Compounds 1 (42.6 mg) and 2 (13.8 mg) were obtained at a retention time of 23.8 and 35.5 min, respectively. 1D- (¹H, 400 MHz, ¹³C, 100 MHz) and 2D-NMR (¹H-¹H COSY, HSQC, HMBC, and NOESY) were measured on a Bruker model digital Advance III 400 NMR for structural elucidation. The NMR data were described in Table 3.

3.8. Preparation of the (R)- and (S)-MTPA Ester Derivatives

To assign the absolute configuration to the molecules, the (S)- and (R)-methoxy- α -(trifluoromethyl)phenylacetyl (MTPA) ester derivatives of 1 and 2 were synthesized in deuterated pyridine (pyridine-*d*₅) from (R)-(+)-MTPA-Cl and (S)-(–)-MTPA-Cl, respectively [18]. Compound 1 (2.0 mg) was dissolved in pyridine-*d*₅ (6 mL) and divided into two NMR tubes (each 1 mL). (R)-MTPA-Cl (4 μ L) was added and reacted at room temperature for 3 h to yield (S)-MTPA ester derivative (1S). Another tube, (S)-MTPA-Cl (4 μ L), was added and reacted at room temperature to yield (R)-MTPA ester derivative (1R), and the ¹H NMR spectrum was recorded on 400 MHz NMR. Similarly (S)- and (R)-MTPA ester derivatives of 2 were prepared as 2S and 2R.

3.9. Assay of ARE-Inducing Activities

HepG2-ARE cells were seeded at a density of 1×10^5 cells/well in 24-well plates for 24 h. The cells were starved for 12 h when they grew to around 80% confluency and were exposed to crude extract, CPC fractions and purified compounds for an additional 24 h. After that, the cells were lysed with 120 μ L of passive lysis buffer (Promega, Madison, WI, USA) in an ice rack and transferred in the 1.5-mL tube. The tubes were centrifuged at 1000 rpm for 3 min. Each supernatant (30 μ L) in the centrifuged tube was reacted with 60 μ L of luciferase assay substrate (Promega, Madison, WI, USA) in the white 96 well plate. Finally, luminescence was measured by an EnSpire multimode plate reader (PerkinElmer,

Waltham, MA, USA). DMSO (below 0.1%) was used as a vehicle, which was a negative control. Sulforaphane (5 μ M) (Calbiochem, Darmstadt, Germany) was used as a positive control. The ARE-luciferase activity was normalized to total protein, determined using BCA protein assay kit with BSA as a standard (Pierce No. 23227).

3.10. Statistical Analysis

All data are reported as means \pm S.E. The statistical significance of differences between treatments was assessed using the Student's *t*-test. A probability value less than 0.05 or 0.01 was considered significant.

4. Conclusions

In the present study, a bioassay-guided isolation method was developed using CPC. To do this, a comprehensive dual-mode CPC was conducted to fractionate bioactive molecules from *L. strychnifolia* root extract. Its higher recovery rate (>95.5%) allowed unbiased bioactivity tests by avoiding irreversible sample adsorption and denaturation that conventional chromatography methods have. After determining active fraction, the constituents were further purified by preparative HPLC to yield linderolide U (**1**) and a new sesquiterpene, linderolide V (**2**) responsible for ARE-inducing activity of *L. strychnifolia* roots. However, as the identified active compounds exist in trace amounts in *L. strychnifolia*, quantitative analysis methods for these compounds are still required. The significance of this study is that the CPC method is an effective screening tool to unearth known or novel bioactive compounds from natural products.

Supplementary Materials: The following are available online, Figure S1: The relative ARE-luciferase activity of *Lindera strychnifolia* extract, Figure S2: CPC chromatogram of crude *L. strychnifolia* extract, Figure S3: HPLC chromatograms and relative ARE-luciferase activity of CPC-fractions (A–R), Figure S4: Comparison of solvent fraction and Fr. B obtained from gradient CPC, Figure S5: ^1H NMR spectrum of **1** (400 MHz) in CD_3OD , Figure S6: ^{13}C NMR spectrum of **1** (100 MHz) in CD_3OD , Figure S7: ^1H - ^1H COSY spectrum of **1** in CD_3OD , Figure S8: HSQC spectrum of **1** in CD_3OD , Figure S9: HMBC spectrum of **1** in CD_3OD , Figure S10: NOESY spectrum of **1** in CD_3OD , Figure S11: ^1H NMR spectra of MTPA esters **1S** and **1R** and $\Delta\delta$ (*S*-*R*) values for (*S*)- and (*R*)-MTPA esters (**1S** and **1R**). Figure S12: HRESI (qTOF) mass spectrum of **1**, Figure S13: ^1H NMR spectrum of **2** (400 MHz) in CD_3OD , Figure S14: ^{13}C NMR spectrum of **2** (100 MHz) in CD_3OD , Figure S15: ^1H - ^1H COSY spectrum of **2** in CD_3OD , Figure S16: HSQC spectrum of **2** in CD_3OD , Figure S17: HMBC spectrum of **2** in CD_3OD , Figure S18: NEOSY spectrum of **2** in CD_3OD , Figure S19: ^1H NMR spectra of MTPA esters **2S** and **2R** and $\Delta\delta$ (*S*-*R*) values for (*S*)- and (*R*)-MTPA esters (**2S** and **2R**), Figure S20: HRESI (qTOF) mass spectrum of **2**.

Author Contributions: Conceptualization, J.H.K. (Ji Hoon Kim), J.-S.J. and C.Y.K.; Data curation, J.H.K. (Ji Hoon Kim), J.H.K. (Jung Hoon Kim) and E.J.J., Y.J.L.; Formal analysis, J.H.K. (Ji Hoon Kim), J.H.K. (Jung Hoon Kim), E.J.J., Y.J.L. and E.M.G.; Funding acquisition, C.Y.K.; Investigation, J.H.K. (Ji Hoon Kim) and E.J.J.; Methodology, J.H.K. (Ji Hoon Kim), J.-S.J., J.H.K. (Jung Hoon Kim) and R.H.S.; Project administration, C.Y.K.; Resources, J.H.K. (Jung Hoon Kim) and E.J.J.; Software, J.H.K. (Ji Hoon Kim) and A.S.S.; Supervision, C.Y.K.; Validation, C.Y.K.; Visualization, J.H.K. (Ji Hoon Kim) and J.-S.J.; Writing—original draft, J.H.K. (Ji Hoon Kim) and J.-S.J.; Writing—review & editing, J.H.K. (Ji Hoon Kim), J.-S.J. and C.Y.K. All authors have read and agreed to the published version of the manuscript.

Funding: This research was supported by the Basic Science Research Program through the National Research Foundation of Korea (NRF-2020R1A2C1009455 and NRF-2020R1A6A1A03042854).

Institutional Review Board Statement: Not applicable.

Informed Consent Statement: Not applicable.

Data Availability Statement: Not applicable.

Conflicts of Interest: The authors declare no conflict of interest.

References

1. Nothias, L.F.; Nothias-Esposito, M.; da Silva, R.; Wang, M.; Protsyuk, I.; Zhang, Z.; Sarvepalli, A.; Leyssen, P.; Touboul, D.; Costa, J.; et al. Bioactivity-Based Molecular Networking for the Discovery of Drug Leads in Natural Product Bioassay-Guided Fractionation. *J. Nat. Prod.* **2018**, *81*, 758–767. [[CrossRef](#)] [[PubMed](#)]
2. Kim, J.H.; Jung, E.J.; Lee, Y.J.; Gao, E.M.; Syed, A.S.; Kim, C.Y. Bioassay-Guided Separation of *Centipeda minima* Using Comprehensive Linear Gradient Centrifugal Partition Chromatography. *Molecules* **2020**, *25*, 3077. [[CrossRef](#)]
3. Wang, D.; Khan, M.S.; Cui, L.; Song, X.Y.; Zhu, H.; Ma, T.Y.; Sun, R. Preparative separation of mangiferin glycosides by high speed counter current chromatography and comparison of their antioxidant and antitumor activities. *RSC Adv.* **2019**, *9*, 4892–4899. [[CrossRef](#)]
4. Santos, J.H.; Almeida, M.R.; Martins, C.I.; Dias, A.C.; Freire, M.G.; Coutinho, J.A.; Ventura, S.P. Separation of phenolic compounds by centrifugal partition chromatography. Continuous separation of cytochrome-c PEGylated conjugates by fast centrifugal partition chromatography. *Green Chem.* **2018**, *20*, 1906–1916. [[CrossRef](#)]
5. da Silva, L.A.L.; Sandjo, L.P.; Fratoni, E.; Moon, Y.J.K.; Dalmarco, E.M.; Biavatti, M.W. A single-step isolation by centrifugal partition chromatography of the potential anti-inflammatory glaucolide B from *Lepidaploa chamissonis*. *J. Chromatogr. A* **2019**, *1605*, 460362. [[CrossRef](#)]
6. Abedini, A.; Chollet, S.; Angelis, A.; Borie, N.; Nuzillard, J.M.; Skaltsounis, A.L.; Reynaud, R.; Gangloff, S.C.; Renault, J.-H.; Hubert, J. Bioactivity-guided identification of antimicrobial metabolites in *Alnus glutinosa* bark and optimization of oregonin purification by Centrifugal Partition Chromatography. *J. Chromatogr. B* **2016**, *1029*, 121–127. [[CrossRef](#)]
7. Zhang, Y.; Liu, C.; Zhang, Z.; Wang, J.; Wu, G.; Li, S.J. Comprehensive separation and identification of chemical constituents from *Apocynum venetum* leaves by high-performance counter-current chromatography and high performance liquid chromatography coupled with mass spectrometry. *Chromatogr. B* **2010**, *878*, 3149–3155. [[CrossRef](#)]
8. Wang, Z.; Hwang, S.H.; Lim, S.S. Comprehensive profiling of minor tyrosinase inhibitors from *Gastrodia elata* using an off-line hyphenation of ultrafiltration, high-speed countercurrent chromatography, and high-performance liquid chromatography. *J. Chromatogr. A* **2017**, *1529*, 63–71. [[CrossRef](#)]
9. Karkoula, E.; Angelis, A.; Koulakiotis, N.S.; Gikas, E.; Halabalaki, M.; Tsarbopoulos, A.; Skaltsounis, A.L. Rapid isolation and characterization of crocins, picrocrocin, and crocetin from saffron using centrifugal partition chromatography and LC-MS. *J. Sep. Sci.* **2018**, *41*, 4105–4114. [[CrossRef](#)]
10. Kim, M.I.; Kim, J.H.; Syed, A.S.; Kim, Y.M.; Choe, K.K.; Kim, C.Y. Application of Centrifugal Partition Chromatography for Bioactivity-Guided Purification of Antioxidant-Response-Element-Inducing Constituents from *Atractylodis Rhizoma Alba*. *Molecules* **2018**, *23*, 2274. [[CrossRef](#)] [[PubMed](#)]
11. Mroczek, T.; Dymek, A.; Widelski, J.; Wojtanowski, K.K. The Bioassay-Guided Fractionation and Identification of Potent Acetylcholinesterase Inhibitors from *Narcissus c.v. 'Hawera'* Using Optimized Vacuum Liquid Chromatography, High Resolution Mass Spectrometry and Bioautography. *Metabolites* **2020**, *10*, 395. [[CrossRef](#)] [[PubMed](#)]
12. Yu, J.; Sun, X.; Zhao, L.; Wang, X.; Wang, X. An efficient method to obtain anti-inflammatory phenolic derivatives from *Scindapsus officinalis* (Roxb.) Schott. by a high speed counter-current chromatography coupled with a recycling mode. *RSC Adv.* **2020**, *10*, 11132–11138. [[CrossRef](#)]
13. Cao, Y.; Xuan, B.; Peng, B.; Li, C.; Chai, X.; Tu, P. The genus *Lindera*: A source of structurally diverse molecules having pharmacological significance. *Phytochem. Rev.* **2016**, *15*, 869–906. [[CrossRef](#)]
14. Liu, Q.; Ahn, J.H.; Kim, S.B.; Lee, C.; Hwang, B.Y.; Lee, M.K. Sesquiterpene lactones from the roots of *Lindera strychnifolia*. *Phytochemistry* **2013**, *87*, 112–118. [[CrossRef](#)] [[PubMed](#)]
15. Sumioka, H.; Harinantenaina, L.; Matsunami, K.; Otsuka, H.; Kawahata, M.; Yamaguchi, K. Linderolides A–F, eudesmane-type sesquiterpene lactones and linderoline, a germacrane-type sesquiterpene from the roots of *Lindera strychnifolia* and their inhibitory activity on NO production in RAW 264.7 cells in vitro. *Phytochemistry* **2011**, *72*, 2165–2171. [[CrossRef](#)] [[PubMed](#)]
16. Liu, Q.; Jo, Y.H.; Kim, S.B.; Jin, Q.; Hwang, B.Y.; Lee, M.K. Sesquiterpenes from the roots of *Lindera strychnifolia* with inhibitory effects on nitric oxide production in RAW 264.7 cells. *Bioorg. Med. Chem. Lett.* **2016**, *26*, 4950–4954. [[CrossRef](#)] [[PubMed](#)]
17. Li, B.; Jeong, G.S.; Kang, D.G.; Lee, H.S.; Kim, Y.C. Cytoprotective effects of lindenyl acetate isolated from *Lindera strychnifolia* on mouse hippocampal HT22 cells. *Eur. J. Pharmacol.* **2009**, *614*, 58–65. [[CrossRef](#)] [[PubMed](#)]
18. Wu, Y.L.; Han, F.; Luan, S.S.; Ai, R.; Zhang, P.; Li, H.; Chen, L.X. Triterpenoids from *Ganoderma lucidum* and Their Potential Anti-inflammatory Effects. *J. Agric. Food Chem.* **2019**, *67*, 5147–5158. [[CrossRef](#)] [[PubMed](#)]
19. Yang, H.J.; Kwon, E.B.; Li, W. Linderolide U, a new sesquiterpene from *Lindera aggregata* root. *Nat. Prod. Res.* **2020**. [[CrossRef](#)] [[PubMed](#)]
20. Kawabata, J.; Tahara, S.; Mizutani, J.; Furusaki, A.; Hashiba, N.; Matsumoto, T. Shizukanolides, Two Sesquiterpenoids from *Chloranthus japonicus* (Chloranthaceae). *Agric. Biol. Chem.* **1979**, *43*, 885–887. [[CrossRef](#)]